

Observation of $(h_{11/2})^2$ neutron alignments in ^{100}Mo , ^{104}Ru , and ^{108}Pd using deep inelastic reactions

P. H. Regan, T. M. Menezes, C. J. Pearson, W. Gelletly, C. S. Purry, and P. M. Walker
Department of Physics, University of Surrey, Guildford, GU2 5XH, United Kingdom

S. Juutinen, R. Julin, K. Helariutta, A. Savelius, P. Jones, P. Jämsen, and M. Muikku
Department of Physics, University of Jyväskylä, Jyväskylä, Finland

P. A. Butler, G. Jones, and P. Greenlees
Oliver Lodge Laboratory, Department of Physics, University of Liverpool, Liverpool, United Kingdom
(Received 7 November 1996)

The transitional nuclei $^{100}_{42}\text{Mo}$, $^{104}_{44}\text{Ru}$, and $^{108}_{46}\text{Pd}$ have been studied as products of binary reactions formed by a $^{86}_{36}\text{Kr}$ beam impinging on a $^{110}_{46}\text{Pd}$ target. The yrast states are observed above the region of the first backbend. In each case this backbend is associated with the breaking of the first neutron $(h_{11/2})^2$ pair. The results are consistent with the predictions of cranked shell model calculations and the systematics of neighboring nuclei. [S0556-2813(97)01904-3]

PACS number(s): 21.10.Re, 23.20.Lv, 25.70.-z, 27.60.+j

I. INTRODUCTION

The nuclei around $Z\sim 44$ and $N\sim 60$ are susceptible to dramatic changes in shape with the addition or subtraction of a small number of nucleons [1]. The population of deformation-driving, two-quasiparticle states can have a polarizing affect on the nuclear shape. Experimentally, the observation of quasiparticle alignments (or “backbending”) can give useful information on the nature of those nucleons lying close to the Fermi surface, allowing the shape of the nuclear mean field to be inferred.

For $Z\sim 44$ and $N\sim 60$, the rotational alignment of both the proton $g_{9/2}$ and neutron $h_{11/2}$ intruder orbitals can give rise to significant increases in aligned angular momentum. For prolate shapes with $\beta_2\sim 0.2$, the Fermi surface lies close to the bottom of the low- Ω , $h_{11/2}$ neutron shell. For the neutron-rich nuclei around $A\sim 105$, these orbitals slope down steeply in energy with increasing prolate deformation. The population of these states has been suggested as the mechanism behind the observation of weakly deformed, prolate, rotational bands in this region [2]. For oblate deformations, at $Z=46$, the low- Ω components of the proton $g_{9/2}$ orbitals are easily aligned and energetically favor collective oblate shapes.

In the lighter ruthenium [3] and palladium nuclei [5,6], backbends are observed in the yrast sequences of the even-even isotopes which have been associated with the population of the prolate driving, two-quasi-neutron, $(h_{11/2})^2$ configuration. However, Aryaeinejad *et al.* [4] suggest that the first band crossing observed in the neutron-rich palladium isotopes, $^{112,114,116}\text{Pd}$, is due to the oblate driving proton $(g_{9/2})^2$ quasiparticle alignment, suggesting an oblate deformed core. It should be noted that in this work the alignment was not observed all the way through the backbend, and so the full increase in alignment could not be extracted. The maximum aligned angular momentum which can be generated by a single pair of proton $g_{9/2}$ orbitals is $8\hbar$, while the neutron $h_{11/2}$ orbitals can generate up to $10\hbar$. Thus for

observed increases in aligned angular momentum of between $9\hbar$ and $10\hbar$, a $(\nu h_{11/2})^2$ assignment would be preferred over a $(\pi g_{9/2})^2$ one.

For neutron-rich nuclei, it is difficult to observe the yrast sequence through the backbend due to the preferential population of neutron-deficient species in fusion-evaporation reactions and the low angular momentum involved in the fission process. The identification of discrete gamma rays from neutron-rich fission fragments [4,7–12] has enabled the observation of low to medium spin yrast states in a number of neutron-rich nuclei around $A=100$ –115. However, in fission source studies, the experimentalist has a limited control over the choice of reaction products, making it difficult to study specific nuclei of interest.

The use of deep inelastic reactions to populate near-yrast states in slightly neutron-rich nuclei is now well established [13–17] and provides an efficient way of studying the yrast states of the most neutron-rich, stable isotopes in the $A\sim 105$ region. In the current work we focus on the evolution of the yrast states as a function of angular momentum in three nuclei $^{100}_{42}\text{Mo}$, $^{104}_{44}\text{Ru}$, and $^{108}_{46}\text{Pd}$, with particular attention to the rotational alignments and what they reveal about the underlying nuclear configurations.

II. EXPERIMENTAL PROCEDURE AND DATA ANALYSIS

In the current work a 5 mg/cm² thick, enriched (99%) ^{110}Pd target on a 20 mg/cm² ^{208}Pb backing was bombarded with a 395 MeV ^{86}Kr beam provided by the K130 cyclotron in the accelerator laboratory at the University of Jyväskylä. Systematic studies of deep inelastic reactions suggest that the nuclei produced with the highest cross section have neutron-to-proton ratios similar to the compound system [18]. Note that the proton-to-neutron ratios for the beam and target nuclei are approximately equal (≈ 0.72) and the $Z:N$ ratios for $^{100}_{42}\text{Mo}$, $^{104}_{44}\text{Ru}$ and $^{108}_{46}\text{Pd}$ are 0.72, 0.73, and 0.74 respectively.

Gamma rays from decays in both the targetlike and projectilelike fragments were measured using an array of 12

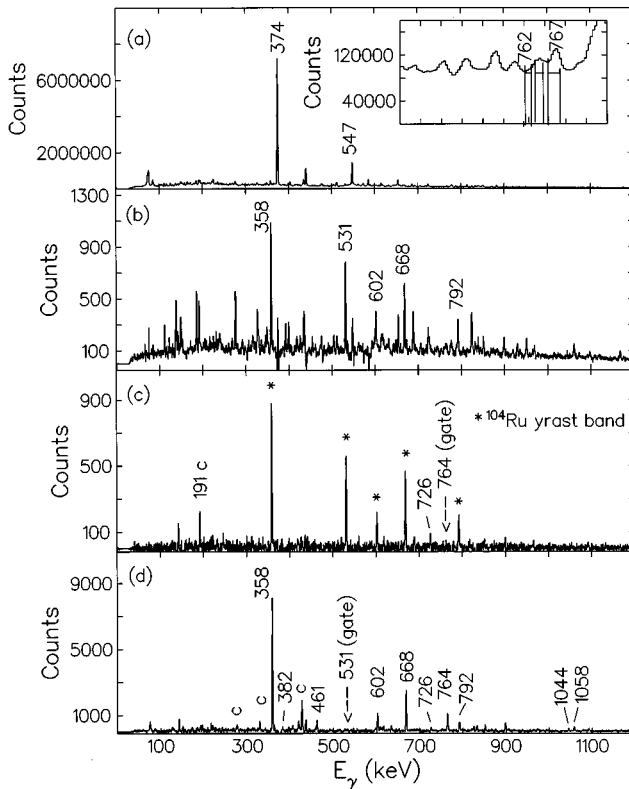


FIG. 1. (a) Total projection of the gamma-gamma coincidence matrix showing the 374 and 547 keV ^{110}Pd lines from Coulomb excitation, (b) background subtracted gate on the 764 keV transition in ^{104}Ru , (c) 764 keV gate with portions of the neighboring 762 and 767 keV gates subtracted, and (d) gate on the 531 keV line.

Compton-suppressed TESSA-type [19], hyperpure germanium detectors. The detectors were placed in four rings of three detectors each, at angles of 38° , 78° , 102° , and 142° to the beam direction. Each individual gamma-ray event was accompanied by a time signal relative to the beam burst which enabled good separation between prompt events (in-beam) and delayed events from isomeric states or β decay.

Data were written to tape for Compton-suppressed gamma-gamma coincidence events. Approximately 4.5×10^8 in-beam, unfolded gamma-gamma events were sorted into the form of a gamma-gamma matrix, from which background-subtracted coincidence gates could be set. Figure 1(a) shows a total projection spectrum for this matrix. Note that the data are dominated by the Coulomb excitation of the ^{110}Pd target.

The data were analyzed using the gamma-ray analysis programs GF2 and ESCL8R [20]. Because of the relatively large number of nuclei formed in this type of reaction, the gates frequently have to be manipulated in order to obtain “clean” (uncontaminated) spectra. Figure 1 shows a typical example using a gamma-gamma coincidence gate set on the 764 keV transition in ^{104}Ru . Clearly, the background-subtracted gate contains many lines which, rather than being in coincidence with the ^{104}Ru transition, are due to the overlap of the tails from peaks either side of the 764 keV transition which are unresolved in the 764 keV gate. When the contributions from these gates are subtracted from the 764 keV gate, the residual spectrum contains only transitions

from ^{104}Ru and the complementary strontium fragments. Typically, each “clean” gate contains lines from the nucleus of interest and also from a number of isotopes from the complementary, projectilelike fragment. In the three nuclei discussed in the present work, ^{108}Pd was accompanied by transitions from $^{84-88}\text{Kr}$, ^{104}Ru was accompanied by transitions from $^{87-90}\text{Sr}$, and ^{100}Mo was accompanied by transitions from $^{91-93}\text{Zr}$. (At the limit of our experimental sensitivity, we do not observe proton evaporation from the binary reaction products.)

III. EXPERIMENTAL RESULTS

The decay schemes for ^{100}Mo , ^{104}Ru and ^{108}Pd , as deduced in the current work, are shown in Fig. 2. Examples of the gamma-gamma coincidence spectra used to construct these decay schemes are shown in Figs. 1 and 3. The intensities quoted are taken from the gamma-gamma coincidence data fitted using the ESCL8R program [20]. This information is summarized for ^{100}Mo , ^{104}Ru , and ^{108}Pd in Tables I, II, and III, respectively. The intensities of the $2^+ \rightarrow 0^+$ transitions were obtained by comparing their intensities as observed in gates set on strong lines in the complementary fragment nuclei. These intensities have been renormalized so that the $2^+ \rightarrow 0^+$ transition in each nucleus has an intensity of 1000 units.

A. Spin and parity assignments

The assignment of transition multiplicities (and thus level spins) in high-spin studies is usually achieved using an angular distribution or directional correlation analysis [21]. In the current work, neither was possible due to (a) the large number of nuclei produced, which means that the singles data are heavily contaminated; (b) a general lack of statistics in the DCO (angle-gated) γ - γ data; and most importantly (c) a destruction of the reaction alignment in the binary breakup process.

The spin assignments given in this work are based on the observed decay characteristics of individual states. Where it exists, we have assumed results from previously published data [22–24] and then made tentative assignments of the spins of previously unobserved states from their decay patterns into the known states. We have made tentative assignments for the level spins using the usual assumption that, typically, near-yrast decays are favored, and thus the assigned spins increase with excitation energy. This assumption is at least partially verified in the present work by the lack of observation of many previously identified nonyrast, low-lying states. We have limited the assigned multiplicities of the decays to either $\Delta I=1$, ($M1/E2$ or $E1$) or $\Delta I=2$, $E2$ transitions (since prompt $M2$ decays in transitional nuclei are rare). In general, the likelihood of a $\Delta I=0$, $J \rightarrow J$ transition has been disregarded on the basis that this implies a nonyrast nature for the decaying state although we note that such decays cannot be ruled out in the present work.

B. Decay scheme of ^{100}Mo

Previous work on this nucleus includes the study of low-spin states following the β^- decay of ^{100}Nb [25], two-

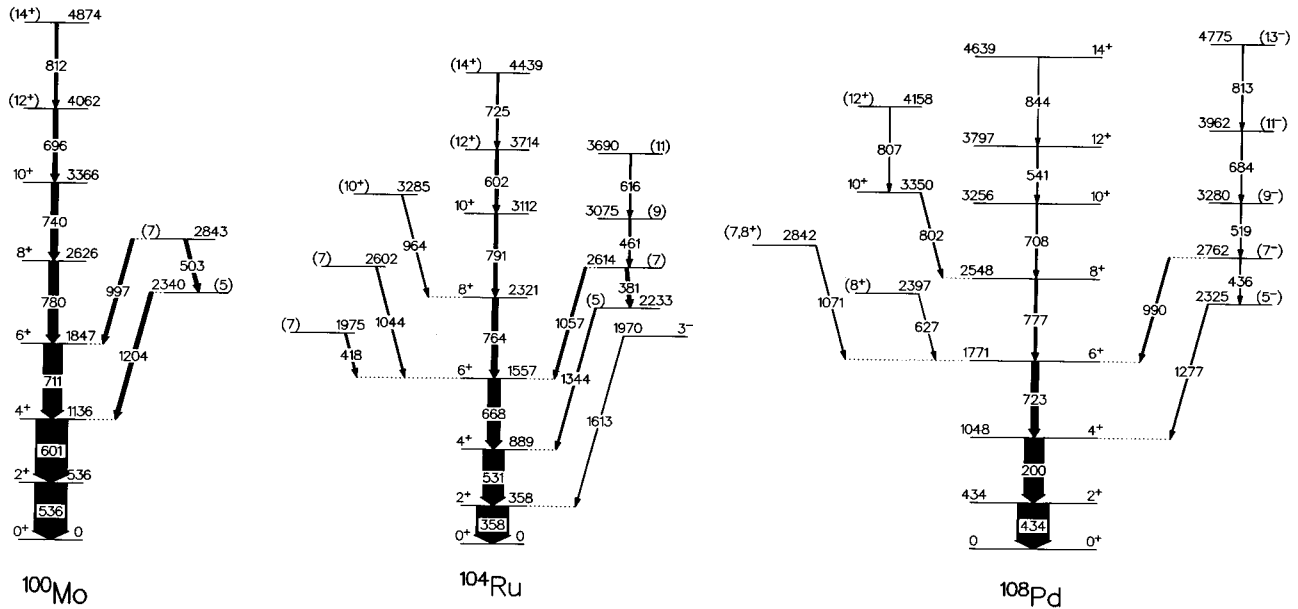


FIG. 2. Partial decay schemes of ^{100}Mo , ^{104}Ru , and ^{108}Pd obtained in the present work.

neutron transfer through the (t,p) reaction [26], and Coulomb excitation [27]. Each of these studies allowed the spin and parity of the yrast 2^+ , 4^+ , and 6^+ states at 536, 1136, and 1848 keV to be confidently assigned. The study by Hook *et al.* [28] using the $^{96}\text{Zr}(^7\text{Li},p2n)^{100}\text{Mo}$ reaction, identified the yrast states up to the 10^+ state at 3368 keV, with the (12^+) state tentatively assigned as lying at 4063 keV. Fission studies reported by Durell [8] suggested a tentative (14^+) state at 4875 keV decaying via an 812 keV transition to this tentative (12^+) state. The excitation energies of these states are confirmed in the present work.

Two previously unreported states at 2340 and 2844 keV have been observed in the current study. The 2340 keV state is observed to decay only to the yrast 4^+ state, restricting likely spins to $5\hbar$ or $6\hbar$ for this state. (A spin/parity of 4^+ for the 2340 keV state is unlikely as one might expect to observe an $E2$ decay to the yrast 2^+ state, yet no such decay is seen in the present study.) By a similar argument, limits of $7\hbar$ and $8\hbar$ can be made for the spin of the 2844 keV state. The observation of the 503 keV transition which links the 2844 and 2340 keV states implies a spin difference of no more than $2\hbar$ between these two levels. On the basis of these arguments, we favor tentative assignments of 5^\pm and 7^\pm for these states, respectively.

C. ^{99}Mo $h_{11/2}$ band

The published data on the $\frac{11}{2}^-$ band in ^{99}Mo [40] extends to a spin- $\frac{19}{2}^-$ state. We have identified a firm candidate for the $(\frac{23}{2}^-)$ member of the decoupled $h_{11/2}$ band in ^{99}Mo which decays via a 845 keV transition (see Fig. 4). The observation of the extension of this band is important in terms of blocking effects and the subsequent interpretation of the backbends in the even-even isotopes (see later).

D. Decay scheme of ^{104}Ru

Levels in ^{104}Ru have previously been studied in β^- decay [29,30], inelastic deuteron scattering [31], Coulomb excitation [23,24,32], massive transfer [3], and the study of fission products [8]. Only the near-yrast states identified during these studies are observed in the current work. The spins and parities of the yrast states up to the 3112 keV level at spin 10^+ have been deduced from Coulomb excitation studies by Stachel *et al.* [23,24].

The yrast positive-parity band is in agreement with the previous work of Haenni *et al.* [3], Stachel *et al.* [23,24], and Durell [8] and has been extended for the first time through the first backbend up to a (14^+) state at 4439 keV. We have assumed that the 602 and 726 keV transitions decaying from the 3714 and 4439 keV states are stretched $E2$ transitions forming the continuation of the yrast band.

A number of previously unobserved, nonyrast states which decay into the yrast sequence have also been identified in the current work. These are the 1975, 2233, 2601, 2614, 3075, 3285, and 3690 keV levels. The spin/parity assignments for these states are discussed below.

1975 keV state. The 1975 keV state has a tentative assignment of $(6^-)\hbar$ or $7\hbar$ on the basis of its only observed decay to the yrast 6^+ state at 1557 keV. If the 1975 keV state had a spin of 8^+ , it would be yrast and one might expect it to have a rather stronger intensity, although such an assignment can not be ruled out in the present work. Similarly, for spin assignments of 6^+ or lower spins, one would expect to see a decay branch to the 4^+ state at 889 keV.

2233, 2614, 3075, and 3690 keV states. The makeup of the decay scheme suggests that these states are all members of a collective structure based on the same intrinsic configuration. (Negative-parity sidebands from the coupling of the $h_{11/2}$ and a $d_{5/2}/g_{7/2}$ orbital are a common feature of the yrast states of this region [22].) From the singular decay of the 2233 keV state to the yrast 4^+ level via the 1344 keV tran-

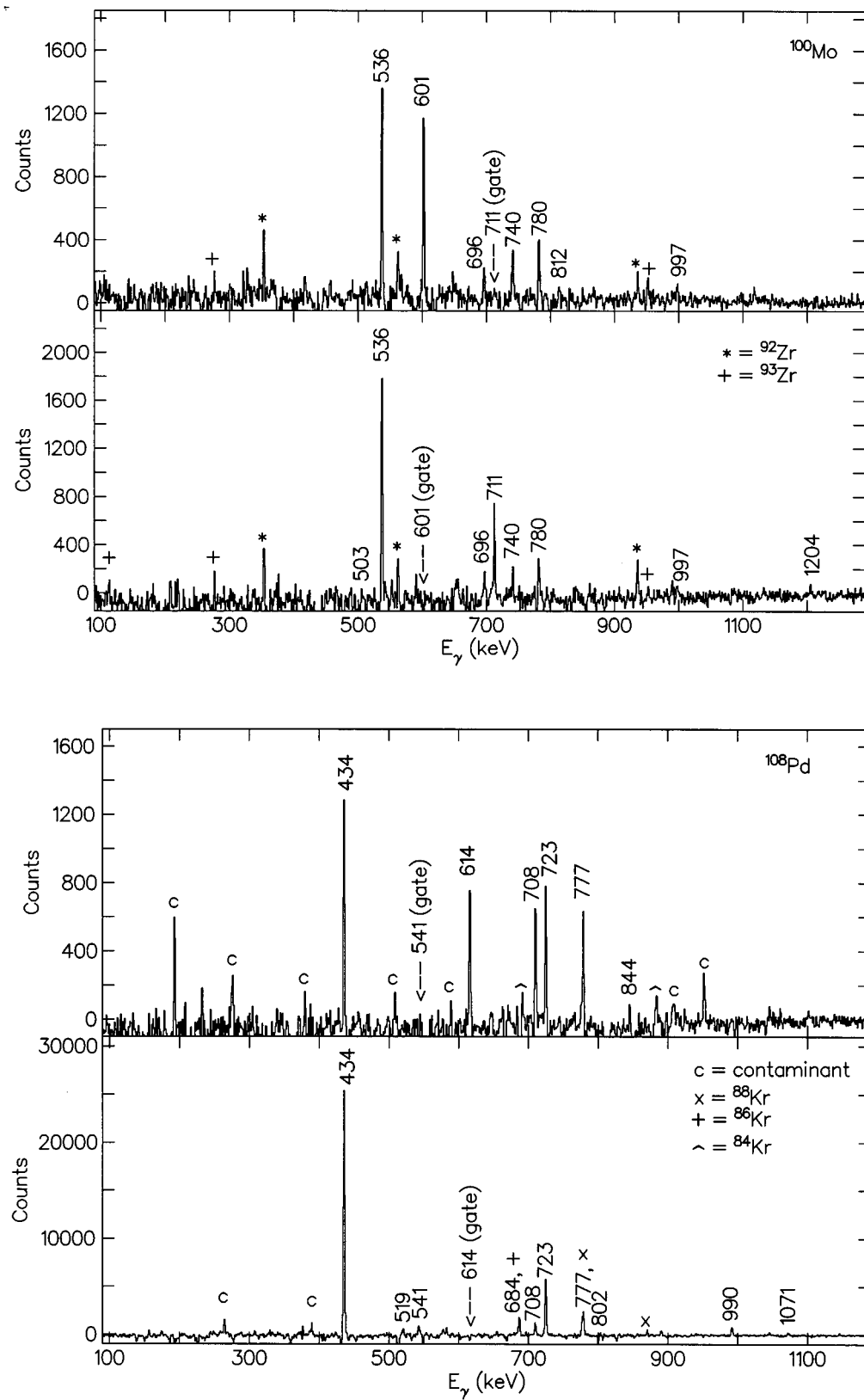


FIG. 3. Examples of coincidence spectra used to obtain the decay schemes for ^{100}Mo and ^{108}Pd in the current work.

sition, tentative spin/parity assignments are restricted to 5^\pm or 6^+ . Similar decay arguments restrict the assignment of the 2614 keV state to 7^\pm or 8^+ and the 3075 keV state to $8\hbar$ or $9\hbar$.

2601 keV state. The observed decay of this state limits its possible spin and parity assignments to 7^\pm or 8^+ . While a 6^- assignment is possible, it is unlikely, particularly since the 2197 keV, 6^+ member of the gamma vibrational band

TABLE I. Transitions identified in ^{100}Mo . Tentative assignments are in parentheses.

E_γ (keV)	Intensity	E_i	E_f	I_i^π	I_f^π
503.3	90(14)	2844	2340	(7)	(5)
535.7	1000(25) ^a	536	0	2 ⁺	0 ⁺
600.6	975(61)	1136	536	4 ⁺	2 ⁺
695.6	128(14)	4063	3368	(12 ⁺)	10 ⁺
711.3	579(38)	1848	1136	6 ⁺	4 ⁺
739.9	210(18)	3368	2628	10 ⁺	8 ⁺
780.3	303(25)	2628	1848	8 ⁺	6 ⁺
812.3	83(14)	4875	4063	(14 ⁺)	(12 ⁺)
996.5	97(14)	2844	1848	(7)	6 ⁺
1204.3	121(21)	2340	1136	(5)	4 ⁺

^aTaken from relative intensity compared to 601 and 711 keV transitions in ^{92}Zr 2⁺→0⁺ (935 keV) gate.

observed by Stachel *et al.* [23,24] is not observed in the present study.

3285 keV state. From the decay of this state via the 964 keV line to the yrast 8⁺ state, likely spin/parity assignments can be restricted to 9[±] or 10⁺.

E. Decay scheme of ^{108}Pd

States upto spin 8⁺ in this nucleus have recently been the focus of a study by Svensson *et al.* [33] using Coulomb excitation. High-spin states up to a tentative (10⁺) state (populated via the decay of fission fragments) have been reported in this nucleus by Durell [8]. The recent study of the near yrast states of ^{108}Pd by Pohl *et al.* [22] using the $^{96}\text{Zr}(^{18}\text{O}, \alpha 2n)$ reaction extended the yrast band up to a tentative spin (18 \hbar) and identified a candidate for the yrast negative-parity band. The decay scheme observed in the present work is consistent with this recent study and spin/parity assignments are taken from that work. In agreement with Ref. [22], the tentative 10⁺ state reported by Durell [8] at 3350 keV is

observed but a lower lying 10⁺ state at 3256 keV which decays via the 708 keV gamma ray is the yrast state for this spin. This has important consequences when deducing the increase in aligned angular momentum through this crossing.

The state at 2842 keV which decays via the 1071 keV transition to the yrast 6⁺ state at 1771 keV has not been previously reported and we assign possible spin/parities for this state of 7[±] or 8⁺.

IV. DISCUSSION AND CSM COMPARISONS

Cranked shell model (CSM) calculations have been performed for all three nuclei using shape parameters obtained from total Routhian surface (TRS) [34] calculations for the lowest energy (0,+) configuration in each case. The calculations for ^{104}Ru are shown in Fig. 5. In all cases, the CSM calculations suggest that the first alignment occurs at a rotational frequency of approximately 0.33 MeV/ \hbar and involves the lowest energy pair of $h_{11/2}$ neutrons (labeled AB). To

TABLE II. Transitions identified in ^{104}Ru . Tentative assignments are in parentheses.

E_γ (keV)	Intensity	E_i	E_f	$I_i^{\pi a}$	I_f^π
358.0	1000(120) ^b	358	0	2 ⁺	0 ⁺
381.0	11(3)	2614	2233	(7,8 ⁺)	(5,6 ⁺)
418.4	50(7)	1975	1557	(6 ⁻ ,7)	6 ⁺
461.3	59(7)	3075	2614	(8,9)	(7,8 ⁺)
530.7	704(91)	889	358	4 ⁺	2 ⁺
601.5	101(13)	3714	3112	(12 ⁺)	10 ⁺
(616.0)	39(5)	(3691)	3075	(9,10,11)	(8,9)
667.9	397(50)	1557	889	6 ⁺	4 ⁺
725.8	24(4)	4439	3714	(14 ⁺)	(12 ⁺)
764.0	198(24)	2321	1557	8 ⁺	6 ⁺
791.5	112(15)	3112	2321	10 ⁺	8 ⁺
964.3	28(4)	3285	2321	(9,10 ⁺)	8 ⁺
1044.3	45(7)	2601	1557	(7,8 ⁺)	6 ⁺
1057.5	75(11)	2614	1557	(7,8 ⁺)	6 ⁺
1344.2	47(7)	2233	889	(5,6 ⁺)	4 ⁺
1613.1	14(3)	1971	358	(3 ⁻)	2 ⁺

^aSee Stachel *et al.* [23,24].

^bTaken from relative intensity compared to 531 and 668 transitions in $^{87,88,89,90}\text{Sr}$ gates.

TABLE III. Transitions identified in ^{108}Pd . Tentative assignments are in parentheses.

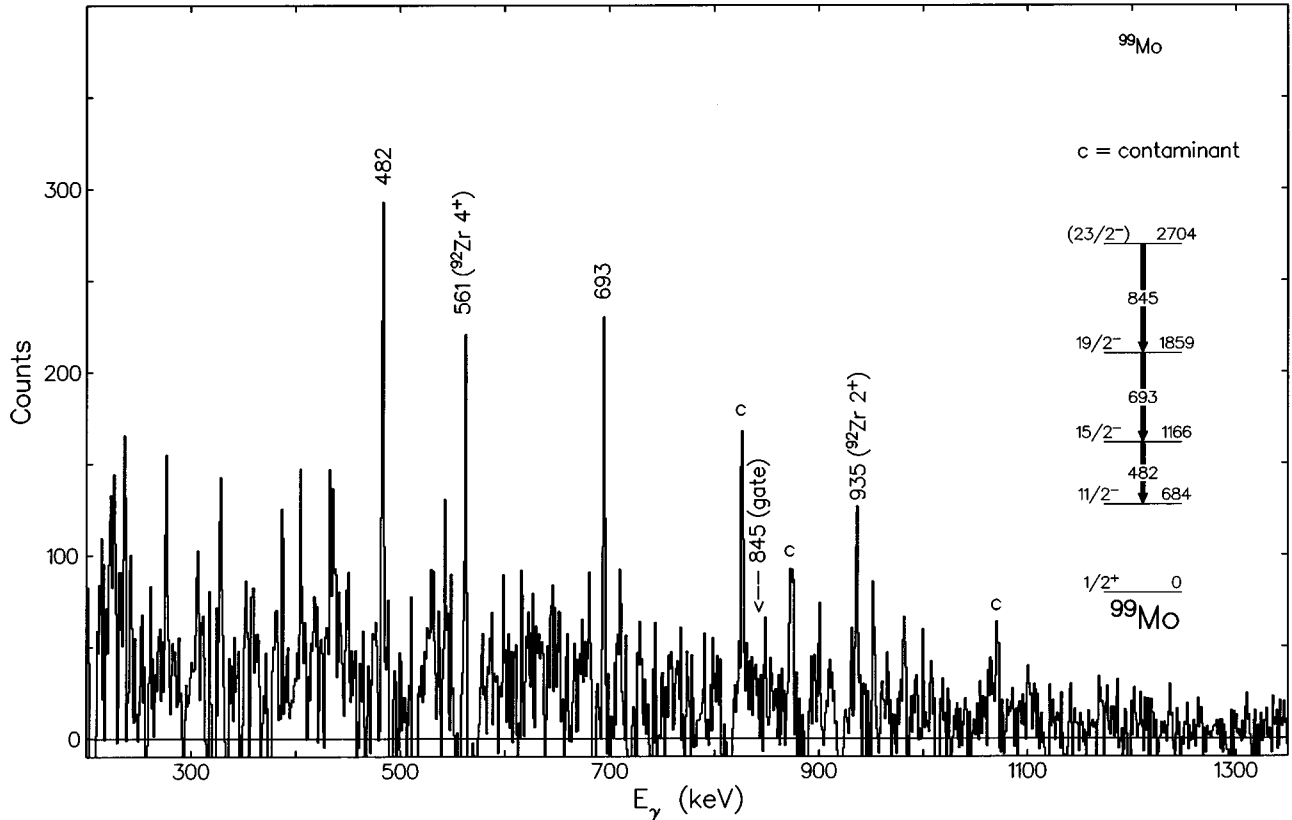
E_γ (keV)	Intensity	E_i (keV)	E_f (keV)	$I_i^{\pi a}$	I_f^π
434.0	1000(80) ^b	434	0	2^+	0^+
435.9	12(2)	2761	2325	$7^{(-)}$	$5^{(-)}$
518.9	19(3)	3280	2761	$9^{(-)}$	$7^{(-)}$
541.2	15(3)	3798	3256	12^+	10^+
614.4	600(55)	1048	434	4^+	2^+
627.3	11(2)	2399	1771	(8^+)	6^+
683.9	18(2)	3964	3280	$11^{(-)}$	$9^{(-)}$
708.3	40(4)	3256	2548	10^+	8^+
723.1	207(18)	1771	1048	6^+	4^+
776.7	77(7)	2548	1771	8^+	6^+
802.4	27(3)	3350	2548	10^+	8^+
807.2	11(2)	4158	3350	(12^+)	10^+
812.9	8(2)	4777	3964	$13^{(-)}$	$11^{(-)}$
843.9	11(2)	4641	3798	14^+	12^+
990.0	45(5)	2761	1771	$7^{(-)}$	6^+
1071.0	18(3)	2842	1771	$(7,8^+)$	6^+
1276.8	28(4)	2325	1048	$5^{(-)}$	4^+

^aSee Pohl *et al.* [22].^bTaken from relative intensity compared to 614 keV transition in total projection.

compare the experimental data with the predictions of the CSM calculations, we have transformed the level energies into excitations in the intrinsic (rotational) frame of the nucleus as described in Ref. [35]. In this analysis, values of $\mathcal{I}_0 = 4\hbar^2/\text{MeV}$ and $\mathcal{I}_1 = 40\hbar^2/\text{MeV}^3$ [36] were used.

A. ^{100}Mo

As Fig. 6 shows, the aligned momentum for the even-spin yrast states for ^{100}Mo increases by approximately $10\hbar$ at a rotational frequency of $0.37 \text{ MeV}/\hbar$. This is consistent with the alignment of the $(h_{11/2})^2$ neutrons as predicted by Mathur

FIG. 4. Gate on the proposed $\frac{23}{2}^- \rightarrow \frac{19}{2}^-$ 845 keV transition in ^{99}Mo .

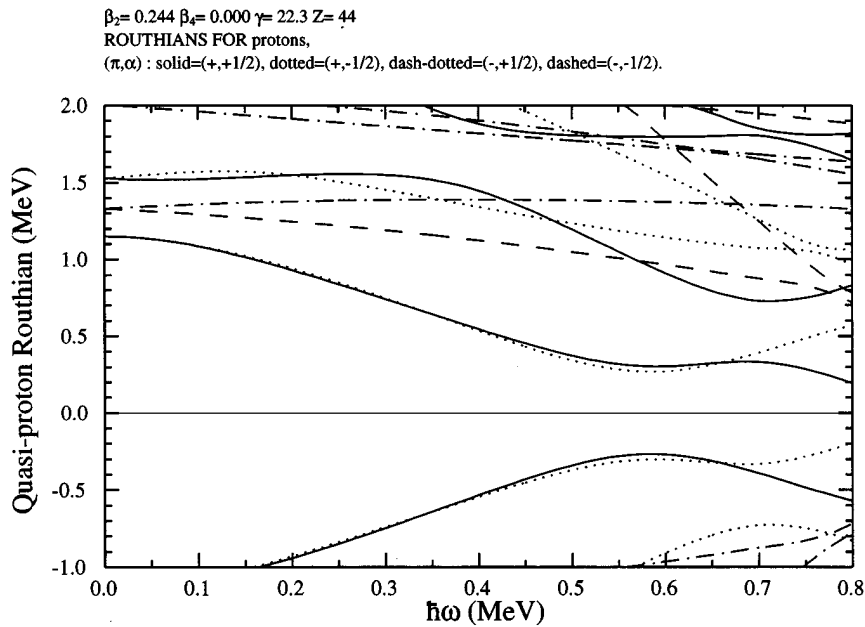
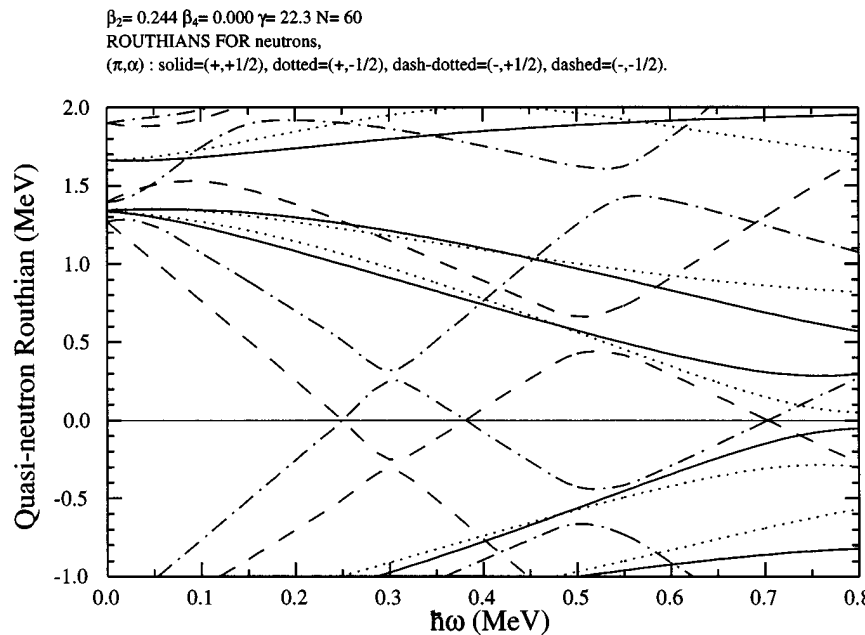


FIG. 5. Cranked shell model calculations for ^{104}Ru assuming triaxiality value of $\gamma=22.3^\circ$.



and Mukherjee [39] and is too large an increase to be explained by the alignment of a $g_{9/2}$ proton pair.

It is useful to compare the alignment observed in ^{100}Mo with that of the one quasi-neutron, $h_{11/2}$ neutron bands in the neighboring odd- N molybdenum isotopes. As Fig. 6 shows, the few states available for the $h_{11/2}$ band in ^{99}Mo show that as in the $h_{11/2}$ bands in ^{103}Ru and ^{107}Pd the first (AB) band crossing is clearly blocked. This blocking effect adds considerable credence to the $(\nu h_{11/2})^2$ interpretation for the first alignment in ^{100}Mo .

One might speculate that the states at 2340 and 2843 keV in ^{100}Mo are negative-parity two-quasiparticle states based

on the coupling of the $h_{11/2}$ neutron orbital with a $d_{5/2}/g_{7/2}$ state. The excitation energy of these states is close to the estimated value of twice the neutron pair gap ($2\Delta_n \approx 2.4$ MeV) and such states are well known in other $N=58$ isotones such as ^{104}Pd and ^{106}Cd [5,42].

B. ^{104}Ru

The observed increase in alignment of $(9 \rightarrow 10) \hbar$ is also consistent with the $(h_{11/2})^2$ crossing and too large for the proton $(g_{9/2})^2$ alignment. This interpretation is supported by the CSM calculations for ^{104}Ru (see Fig. 5) which predict the

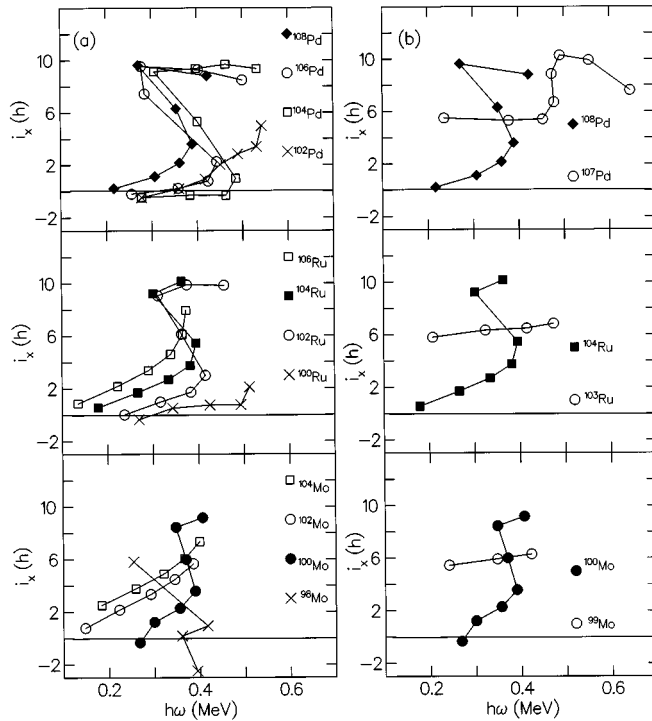


FIG. 6. Alignments for the (a) even isotopes of palladium ($Z=46$), ruthenium ($Z=44$), and molybdenum ($Z=42$) and (b) comparison with the $h_{11/2}$ neutron bands in the respective odd- A neighbors. In all cases, the Harris parameters used were $\mathcal{I}_0=4 \hbar^2/\text{MeV}$ and $\mathcal{I}_1=40\hbar^2/\text{MeV}^3$. The data for these points come from the present work and Refs. [3,5,6,8,22,37,38,40].

$(\nu h_{11/2})^2$ alignment (AB) to occur at a frequency of approximately $0.3 \text{ MeV}/\hbar$. The alignment for the $\frac{11}{2}^-$ band in ^{103}Ru [3] shows this AB band crossing to be blocked [see Fig. 6(b)], again consistent with the $(\nu h_{11/2})^2$ alignment interpretation for ^{104}Ru . The excitation energy of the first $\frac{11}{2}^-$ state lies at only 209 keV [41] in ^{105}Ru (compared to 434 keV in ^{103}Ru), but unfortunately no states are known in the band built on this state; so the alignment for this band cannot be deduced. However, the lowering of the energy of the yrast $\frac{11}{2}^-$ state with increasing neutron number is consistent with the $h_{11/2}$ neutron orbital lying close to the Fermi surface for ^{104}Ru .

The states at 1995, 2233, 2602, and 2614 keV are all at excitation energies consistent with two-quasiparticle states, but in the absence of firm spin/parity assignments, no further interpretation can be made. The tentative (10^+) state at 3285 keV is a candidate for the continuation of the yrare, quasivibrational ground state configuration after the first band crossing.

C. ^{108}Pd

It has been suggested that there is change from prolate to oblate deformation in the palladium isotopes [4] with oblate shapes preferred for neutron numbers 64 and above. Aryaeinejad *et al.* [4] have argued oblate deformations for $^{112,114,116}\text{Pd}$ on the basis of the observed rotational frequencies of the first alignment for these nuclei, which occurs at $\omega \sim 0.35 \text{ MeV}/\hbar$. The authors of Ref. [4] suggest that this is consistent with the $(\pi g_{9/2})^2$ crossing which is predicted to occur at a lower frequency than the $(\nu h_{11/2})^2$ alignment for oblate shapes. (However, this situation is reversed for weakly deformed prolate deformations.) Unfortunately, the backbends observed in $^{112,114,116}\text{Pd}$ do not progress through the full alignment and thus the total increase in aligned angular momentum through these backbends has not yet been established.

In ^{108}Pd , the CSM calculations suggest that the first alignment is due to the prolate driving, low- Ω $(h_{11/2})^2$ neutron configuration [22], consistent with the observed gain in angular momentum of $(9 \rightarrow 10)\hbar$. As in the ^{100}Mo and ^{104}Ru yrast bands, this increase in aligned angular momentum is too large to be accounted for by the proton $(g_{9/2})^2$ alignment. As Fig. 6(b) shows, the first alignment in ^{108}Pd is blocked in the one-quasineutron $\frac{11}{2}^-$ band in ^{107}Pd , consistent with a $(h_{11/2})^2$ alignment in ^{108}Pd .

V. SUMMARY AND CONCLUSIONS

The yrast states of the β -stable nuclei ^{100}Mo , ^{104}Ru , and ^{108}Pd have been studied to medium spins using deep inelastic collisions. In each case, the yrast sequence extends past the first band crossing with an increase in aligned angular momentum of approximately $10\hbar$. This pattern is well reproduced by cranked shell model calculations and the systematics of the neighboring nuclei, all of which suggest that the neutron $(h_{11/2})^2$ alignment is energetically favored over the ground state configurations at spins of $10\hbar$ and above.

ACKNOWLEDGMENTS

The authors gratefully acknowledge R. Darlington for making the target and the crew of the Jyväskylä cyclotron. We are very grateful to Dr. Ramon Wyss of the Manne Siegbahn Institute, Stockholm, Sweden for providing us with the TRS and CSM calculations. This work benefited from useful discussions with Dr. O Burglin. One of us (T.M.M.) acknowledges support from the JNICT (Portugal) under the PRAXIS XXI program, Project No. PRAXISS XXI/BD/5665/1995. This work is also supported by grants from the Engineering and Physical Sciences Research Council (UK), the European Union, and the British Council's Finnish-British Academic Research Collaboration Scheme.

[1] *Nuclear Structure of the Zirconium Region*, edited by J. Eberth, R. Meyer, and K. Sistemich (Springer-Verlag, Berlin, 1988).

[2] I. Thorslund *et al.*, Nucl. Phys. **A564**, 285 (1993).

[3] D. R. Haenni, H. Dejbakhsh, R. P. Schmitt, and G. Mouchaty, Phys. Rev. C **33**, 1543 (1986).

[4] R. Aryaeinejad *et al.*, Phys. Rev. C **48**, 566 (1993).

[5] J. A. Grau, L. E. Samuelson, F. A. Rickey, P. C. Simms, and G. J. Smith, Phys. Rev. C **14**, 2297 (1976).

[6] A. O. Macchiavelli, J. Burde, R. M. Diamond, C. W. Beausang, M. A. Deleplanque, R. J. McDonald, F. S. Stephens, and J. E. Draper, Phys. Rev. C **38**, 1088 (1988).

- [7] J. Shannon *et al.*, Phys. Lett. B **336**, 136 (1994).
- [8] J. L. Durell, in *Proceedings of the International Conference on Spectroscopy of Heavy Nuclei*, Crete, 1989, edited by J. F. Sharpey-Schafer and L. D. Skouras, IOP Conf. Proc. No. 105 (Institute of Physics, London, 1990), p. 307.
- [9] M. A. C. Hotchkis *et al.*, Phys. Rev. Lett. **64**, 3123 (1990).
- [10] M. A. C. Hotchkis *et al.*, Nucl. Phys. **A530**, 111 (1991).
- [11] Q. H. Lu *et al.*, Phys. Rev. C **52**, 1348 (1995).
- [12] K. Butler-Moore *et al.*, Phys. Rev. C **52**, 1339 (1995).
- [13] M. W. Guidry *et al.*, Phys. Lett. **163B**, 79 (1985).
- [14] H. Takai *et al.*, Phys. Rev. C **38**, 1247 (1988).
- [15] R. Broda, M. A. Quader, P. J. Daly, R. V. F. Janssens, T. L. Khoo, W. C. Ma, and M. W. Drigert, Phys. Lett. B **251**, 245 (1990).
- [16] B. Fornal *et al.*, Phys. Rev. C **49**, 2413 (1995).
- [17] B. Fornal *et al.*, Acta Phys. Pol. B **26**, 357 (1995).
- [18] H. Freiesleben and J. V. Kratz, Phys. Rep. **106**, 1 (1984).
- [19] J. Simpson, M. Bates, C. Brookes, and P. J. Nolan, Nucl. Instrum. Methods Phys. Res. A **269**, 209 (1988).
- [20] D. Radford, *Proceedings of the International Seminar on the Frontier of Nuclear Spectroscopy*, edited by Y. Yoshizawa, H. Kusakari, and T. Otsuka (World Scientific, Singapore, 1993), p. 229; Nucl. Instrum. Methods Phys. Res. A **361**, 297 (1995).
- [21] K. S. Krane, R. M. Steffen, and R. M. Wheeler, Nucl. Data Tables **11**, 351 (1973).
- [22] K. R. Pohl, P. H. Regan, J. E. Bush, P. E. Raines, D. P. Balamuth, D. Ward, A. Galindo-Uribarri, V. P. Janzen, S. M. Mullins, and S. Pilotte, Phys. Rev. C **53**, 2682 (1996).
- [23] J. Stachel, N. Kaffrell, E. Grosse, H. Emling, H. Folger, R. Kulessa, and D. Schwalm, Nucl. Phys. **A383**, 429 (1982).
- [24] J. Stachel *et al.*, Nucl. Phys. **A419**, 589 (1984).
- [25] G. Menzen, K. Systemich, G. Lhersonneau, and H. Gietz, Z. Phys. A **327**, 119 (1987).
- [26] M. A. Choudhury, W. Booth, and R. N. Glover, Nuovo Cimento A **99**, 701 (1988).
- [27] S. J. Mundy, W. Gelletly, J. Lukasiak, W. R. Phillips, and B. J. Varley, Nucl. Phys. **A441**, 534 (1985).
- [28] D. Hook, J. L. Durell, W. Gelletly, J. Lukasiak, and W. R. Phillips, J. Phys. G **12**, 1277 (1986).
- [29] K. Sümmerer, N. Kaffrell, H. Otto, P. Peuser, and N. Trautmann, Z. Phys. A **287**, 287 (1978).
- [30] K. Sümmerer, N. Kaffrell, and N. Trautmann, Nucl. Phys. **A308**, 1 (1978).
- [31] J. Rekestad and P. O. Tjom, J. Phys. G **3**, 411 (1977).
- [32] S. Landsberger, R. Lecomte, P. Paradis, and S. Monaro, Phys. Rev. C **21**, 588 (1980).
- [33] L. E. Svensson, C. Fahlander, L. Hasselgren, A. Bäcklin, L. Westberg, D. Cline, T. Czosnyka, C. Y. Wu, R. M. Diamond, and H. Kluge, Nucl. Phys. **A584**, 547 (1995).
- [34] W. Nazarewicz, R. Wyss, and A. Johnson, Nucl. Phys. **A503**, 285 (1989).
- [35] R. Bengtsson and S. Frauendorf, Nucl. Phys. **A314**, 27 (1979).
- [36] S. M. Harris, Phys. Rev. **138**, B509 (1965).
- [37] M. A. J. de Voigt, J. F. W. Jansen, F. Bruning, and Z. Sujkowski, Nucl. Phys. **A270**, 141 (1976).
- [38] C. M. Lederer, J. M. Jaklevic, and J. M. Hollander, Nucl. Phys. **A169**, 449 (1971).
- [39] T. Mathur and S. Mukherjee, Phys. Rev. C **44**, 909 (1991).
- [40] J. Dubuc, G. Kajrys, P. Larivière, S. Pilotte, W. Del Bianco, and S. Monaro, Phys. Rev. C **37**, 954 (1988).
- [41] D. De Frenne and E. Jacobs, Nucl. Data Sheets **68**, 935 (1993).
- [42] P. H. Regan *et al.*, Nucl. Phys. **A586**, 351 (1995).